



## STRENGTHENING OF TUBULAR STEEL COMPRESSION MEMBERS WITH FIBER-REINFORCED POLYMERS (FRP)

Ahmed Mostafa El- kholy<sup>1</sup>, Yomna Ahmed Mohammed<sup>2</sup>,  
Sherif Ahmed Mourad<sup>3</sup> and Ayman Ahmed Shaheen<sup>4</sup>

<sup>1</sup>Lecturer of Structural Engineering, Faculty of Engineering, Fayoum University, Egypt.

<sup>2</sup>Teaching Assistant & M.Sc. Candidate, Faculty of Engineering, Fayoum University, Egypt.

<sup>3</sup>Professor of Steel Structures and Bridges, Faculty of Engineering, Cairo University, Egypt.

<sup>4</sup>Professor of Reinforced Concrete Structures, Faculty of Engineering, Fayoum University, Egypt.

### ملخص البحث:

على الرغم من الاستخدام المنتشر لمركبات البوليمر المقوى بالألياف في تدعيم المنشآت الخرسانية فإنها تستخدم في تطبيقات قليلة في المنشآت المعدنية وخصوصاً في القطاعات الأنبوبية. إن العناصر الصلب الأنبوبية المعرضة لقوى ضغط يُحتمل أن تتعرض لانبعاج جزئي موضعي مثل انبعاج قدم الفيل أو انبعاج كلي. يقدم هذا البحث تحليلاً عددياً غير خطي ثلاثي الأبعاد لدراسة سلوك الانبعاج الإنشائي للعناصر الصلب الأنبوبية والمدعمة بمركبات البوليمر المقوى بالألياف تحت تأثير قوى ضغط محوري. تم تمثيل عيوب الصناعة في النموذج من انبعاج جزئي متغير على امتداد طول وقطر الاسطوانة أو انبعاج كلي مبدئي لتمثيل نمطي الانبعاج المدروسين في هذا البحث. تم تقييم نتائج نماذج التحليل العددي من خلال مقارنتها بنتائج معملية في بحوث سابقة. وكشفت النتائج العددية توافقاً كبيراً بينها وبين القياسات التجريبية.

### ABSTRACT

Although fiber reinforced polymers (FRP) have been widely used in strengthening of concrete structures, there are few applications to steel structures, especially to tubular sections. Tubular steel elements exposed to axial compression are likely to be subjected to local buckling mode such as elephant's foot buckling mode or overall buckling mode. This paper presents 3-D nonlinear finite element analysis to investigate the buckling behavior of tubular steel members strengthened with fiber reinforced polymer FRP under uniaxial compression. Imperfections were introduced to simulate the two types of buckling studied in this paper; elephant's foot and overall buckling modes. The finite element models' results were verified and evaluated by comparing them with the experimental ones. The numerical results revealed good agreement with available experimental measurements.

**Keywords:** Elephant's foot buckling mode, Overall buckling, Strengthening, Tubular steel members, uniaxial compression, FRP.

### 1. INTRODUCTION

Steel hollow sections are one of the most versatile and efficient forms for construction and mechanical applications. Many of the strongest and most impressive structures in the world today would not have been possible without hollow sections. High strength per unit weight is considered to be one of the most important characteristics of the hollow steel sections [1,2]. Buckling is the common failure of the hollow steel sections, whether local buckling such as elephant's foot buckling mode or overall buckling. The elephant's foot buckling mode is a typical local buckling mode of circular hollow steel tubes which appears as an outward bulge near the ends of the tube [3]. It can occur due

to outward imperfection in addition to axial compression alone , in combination with cyclic lateral loading or in combination with internal pressure. The same mode of buckling may occur in square hollow sections under axial load and it is called roof mechanism [4,5]. It commonly occurs at the mid height of the specimens. The overall buckling mode is also a common mode of buckling for the hollow steel sections due to axial load in addition to small out-of-straightness imperfection in the specimen. These previous imperfections are categorized as geometric imperfection. It means that either the steel section itself has slightly geometric deviation from the ideal shape. This imperfection arises during the manufacturing of the steel element [6,7]. Also, material imperfections exist in steel in form of point, line, planer, and volume defects [8].

Strengthening of steel structures is commonly carried out by steel plates [9,10]. Because steel plates weigh heavily and can be corroded, they have been replaced with fibers reinforced polymers composite (FRP). In addition to superior thermo-mechanical properties, FRP composites have many advantages over conventional materials such as high strength, long service life, impact resistance and excellent corrosion resistance [11-13]. Therefore, FRP may be used to strengthen hollow steel sections to improve the structural buckling behavior of the steel elements.

Research work on strengthening of tubular steel compression members is very limited. Batikha et al. [14] presented numerically a new method of strengthening tubular sections to resist elephant's foot buckling. This method involves the use of a small amount of FRP in the critical location of the tube and this method had proven to be effective in eliminating the problem and increase the buckling strength. Haedir and Zhao [15] presented an experimental study to evaluate the performance of externally bonded carbon fiber (CFRP) in strengthening circular steel tubular short columns under axial load to resist the elephant's foot buckling. The results confirmed that enhancement of the axial section capacity would be possible by strengthening the tubular column with CFRP. Shaat and Fam [9] provided an experimental study to investigate the behavior of short square hollow steel sections strengthened with CFRP under axial load. The predominated modes of buckling for the short columns were elephant's foot buckling. The results showed that the maximum strength gain of 18% was achieved with two transverse CFRP layers. There are other researches that study the same modes of buckling, but the loads were not limited to the axial load. Nishino and Furukawa [16] conducted cyclic loading tests on a circular tube beam-column strengthened with CFRP sheet using a loading system that causes double curvature bending. They found that CFRP can increase the deformation capacity of circular tube beam-columns and the carbon fiber prevented local ring-type buckling (elephant's foot buckling mode).

For overall buckling, Shaat and Fam [9] provided an experimental study to investigate the behavior of long square hollow steel sections strengthened with CFRP under axial load. The predominated modes of buckling for the long columns were overall buckling. The maximum strength gain was 23% with three longitudinal CFRP layers applied on four sides. Gao et al. [10] conducted an experimental study to investigate the effect of strengthening tubular steel sections with carbon fiber reinforced polymers (CFRP) on the overall buckling behavior. They concluded that externally bonded longitudinal CFRP sheets were effective in increasing the axial strength and stiffness of slender braces.

## 2. Experimental Studies

In this paper, two experiment studies were used to verify the finite element models mentioned latterly in this study. The first one studied the elephant's foot buckling mode on hollow steel tube under axial load [11]. The second one studied the overall buckling mode on hollow steel tube under axial load [10].

### 2.1 The elephant's foot buckling

Teng and Hu [11] presented experimental and numerical studies to explore the benefit of strengthening with FRP on the behavior of circular steel hollow sections. Four steel tubes with and without strengthening were tested on this study with outer diameter equal 165 mm, length of the tube equal 450 mm and thickness equal 4.2 mm. The type of fiber used in this study was glass fiber reinforced polymers (GFRP). The mechanical properties of the steel and the fiber used in this study are shown in Table (1). Compression tests were performed for all the tubes with displacement control machine. **Figure (1)** shows the failure modes of the four tubes. The failure mode of the control steel tube (without fiber) was outward buckling around the circumference (**Fig. 1-a**). This type of buckling is known as elephant's foot buckling mode. The failure of the tube strengthened with 1-layer of GFRP involved outward buckling near the ends of the tube as in **Fig. (1-b)** and some inward buckling, but the outward buckling was the predominated mode of buckling. In the tube strengthened with 2- layers of GFRP, the inward buckling became more important than the previous tube besides the outward buckling near the ends of the tube and when 3-layers of GFRP were used, the outward buckling near the ends of the tube almost disappeared and the inward buckling became the predominated mode of buckling. From previous, it can be concluded that the increase in fiber's layers decreased the outward buckling.

Table (1) Mechanical properties of steel and GFRP for elephant's foot buckling models

	Elastic modulus	Ultimate strength	Ultimate strain
Steel	201 GPa	370 MPa	0.347
GFRP	80.1 GPa	1825.5 MPa	0.0228



a- No fiber



b- 1-Layer GFRP

Fig. 1: failure modes of steel tubes (Teng and Hu, 2007)

## 2.2 The overall buckling

Gao et al. [10] conducted an experimental study supported by a numerical study to investigate the effect of strengthening tubular steel sections with carbon fiber reinforced polymers (CFRP) on the overall buckling behavior. Seven steel tubes with and without CFRP jacket were tested on this study with outer diameter equal 88.9 mm, length of the tube equal 2.4 m and thickness equal 4 mm. The mechanical properties of the steel and the CFRP used in this study were shown in Table (2). Compression tests were carried out on the tubes with load control machine. Lubricated cylindrical bearing (**Fig. 2**) was used at the bottom end of the tube to allow rotation. In the control steel tube, the main cause of failure was the overall buckling in addition to secondary local buckling in the compression side at or near the middle of the tube. For strengthening tubes, the overall buckling was not the case of failure. The secondary local buckling of the compression side of the tube which was associated with crushing of CFRP layers was the main cause of failure in these tubes.

Table (2) Mechanical properties of steel and CFRP for overall buckling models

	Elastic modulus	Ultimate strength	Ultimate strain
Steel	201 GPa	490 MPa	0.347
CFRP	230 GPa	300 MPa	0.015



Fig. 2: Lubricated cylindrical bearing (Gao et al., 2013)

### 3. Finite Element Analysis

Three-dimensional nonlinear analysis was conducted to achieve fully understand of the buckling behavior of tubular steel sections under axial load. The 3-D models were produced by ANSYS program [17]. Two groups of models were established to simulate two modes of buckling; elephant's foot buckling mode (model I) and overall buckling mode (model II). These models were verified by comparing their results with the experimental results which were mentioned previously in section (2). More details on the models may be found in Ref. [18].

#### 3.1 Elephant foot's buckling models

##### 3.1.1 General

Two ANSYS models were generated to simulate the specimens at the experimental study [11], without fiber and with 1-layer of GFRP. The models had the same dimensions of the experimental specimens. Both geometric and material nonlinearities were considered in the models. The arc length method was used to follow the nonlinear load deformation path. Shell 93 and Shell 181 were chosen to represent the steel tube. Shell 93 is 8-node structural shell with six degree of freedom at each node (three translations and three rotations). It is suitable for rounded shell model. Shell 181 is a 4-node strain shell element with six degree of freedom (three translations and three rotations). It is suitable for analyzing thin to moderately-thick shell structures [17]. Beam 4 was used to represent the fiber sheets. It is 3-D elastic beam with six degrees of freedom and with tension, compression, torsion, and bending capabilities [17].

The tube was divided as 5 mm × 10 mm. The longer part of the element lied over the circumferential direction of the tube because the deformations of the tube in the circumferential direction were generally small. The stress strain curve which used in the model is shown in **Fig. (3-a)**.

##### 3.1.2 Boundary condition

In the experimental study, the steel tube was in contact with stiff loading plates at both ends. For that, each node at the top and bottom ends of the tube was fully fixed in the numerical models except the axial displacement of the top end of the tube was left unrestrained to allow the application of load.

##### 3.1.3 Imperfection of the steel tubes

Because of the imperfection in the experimental steel tube, the buckling appeared at one end of the tube. Geometric imperfection was included in the finite element model for steel tubes to match the observations of buckling in the experimental study. To guide the tube into deformations which should be almost like the deformation from the experiment, an axisymmetric outward imperfection was applied as a local outward bulge in the form of a half-wave sine curve along the meridian, and was added near the top end of the tube in the model of control steel tube. The half-wave length of the sine curve was taken equal 31.75 mm and the imperfection amplitude was taken as 0.01 mm. For the model representing strengthened steel tube with 1-layer of GFRP, a non-axisymmetric geometric imperfection was included in the finite element model (**Fig. 3-b**). The imperfection model proposed by Teng and Hu [11] was adopted after changing the coordinate to radial in this equation:

$$DR_i = w_o \times \sin\left(\frac{\pi \times (Z_t - NZ_i)}{L}\right) \times \cos\left(\frac{n \times NY_i \times \pi}{180}\right) \quad (1)$$

where  $w_o$  is the amplitude of the imperfection (0.01 mm),  $Z_t$  is the total length of the tube (450 mm),  $L$  is the half-wave length of the sine curve in the longitudinal direction from the top of the tube (31.75 mm), and  $n$  is the number of circumferential waves of the imperfection (2). The sequence of applying the imperfection was as the flow chart shown in **Fig. (3-c)**.

## 3.2 Overall buckling models

### 3.2.1 General

Three ANSYS models were used to simulate the test tubes of the experimental study [10], without fiber, with 2-layers of CFRP, and with 4-layers of CFRP. Both geometric and material nonlinearities were considered in the models. Shell 93 was chosen to represent the steel tube and Beam 4 was used to represent the fiber sheets because of their properties (refer to section 3.1.1).

The tube was divided into a grid 2.5 mm × 10 mm (the shorter part in the circumferential direction as this mesh was suitable for the dimensions of the tube). The stress strain curve which was used in the model is shown in **Fig. (4-a)**. Full Newton-Raphson was chosen as a solver in these models [18].

### 3.2.2 Boundary condition

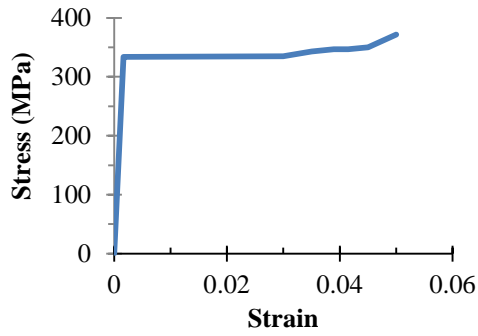
The constraint at the ends of the tube was hinged in the experimental study [10]. For reaching the behavior of hinged constrain, a cap made from number of rigid links was added to the model (**Fig. 4-b**). The element (Link 8) was used to form the rigid links. It is a uniaxial tension-compression element with three degrees of freedom at each node (transitions in the three directions) [17]. To minimize the axial deformation in the cap's links, linear steel material was defined with extremely high young's modulus for the material of links.

### 3.2.3 Imperfection of the steel tubes

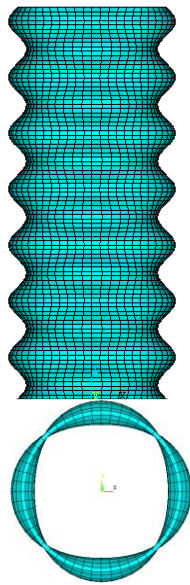
A small displacement was applied at mid-span in X-direction (**Fig.4-c**) to verify the imperfection and to match experimental observations in verification paper [10]. An equation was applied to simulate the imperfection. This equation was as following:

$$DX_i = e_o \times \sin\left(\frac{\pi \times NZ_i}{L}\right) \quad (2)$$

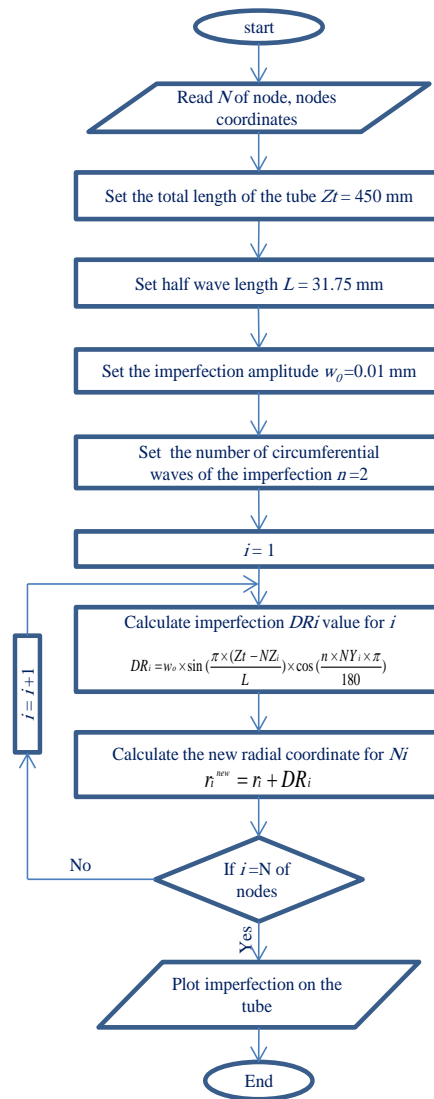
where  $e_o$  is the initial imperfection and it was used in two values, 0.5 mm and 2.4 mm and  $L$  is the length of the tube (2400 mm). The imperfection was applied by using the flow chart shown in **Fig. (4-d)**.



a- stress-strain curve

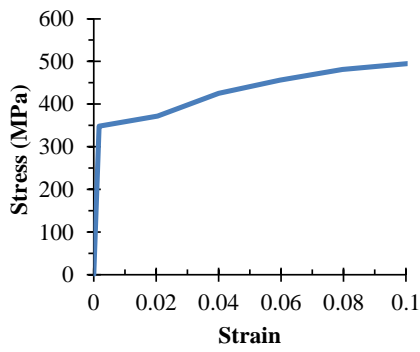


b- Geometric imperfection assumed for FRP confined steel tube (scale factor =1000)

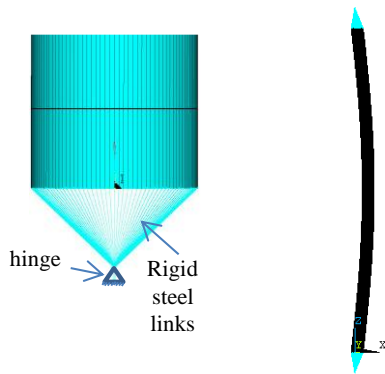


c- Flow chart for the application of the imperfection

Fig. 3: Material and geometric nonlinearities in the elephant's foot model

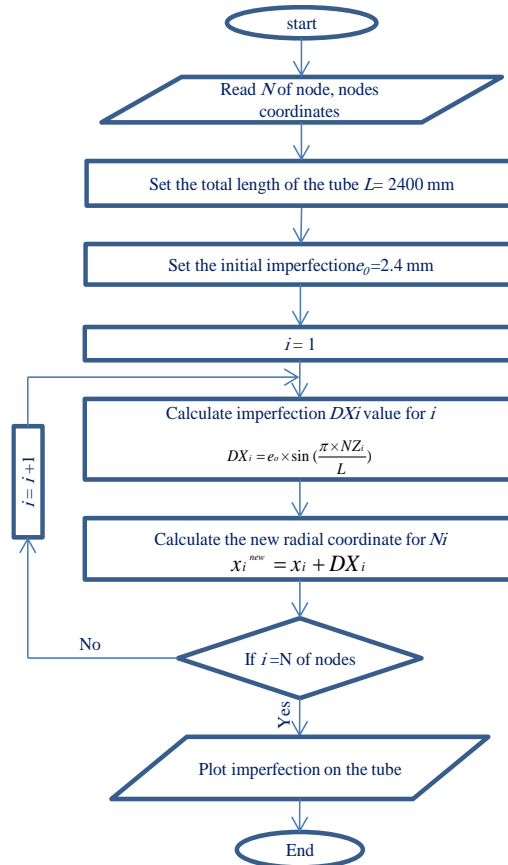


a- stress-strain curve



b- boundary conditions

c- Geometric imperfection assumed for FRP confined steel tube (scale factor =200)



d- Flow chart for the application of the imperfection

Fig. 4: Material and geometric nonlinearities and boundary condition in the overall buckling model

## 4. Results

The results from the previous models were verified and evaluated by comparing them with the experimental results

### 4.1 Elephant foot's buckling models

**Figure (5)** illustrates the hoop strain plotted on the deformed shape and buckling shape of experimental and numerical control steel tube and strengthened steel tube with 1-layer GFRP, respectively. The figure shows that the behavior obtained from ANSYS model is very close to the experimental results. Also, it shows the effect of fiber jacket on the steel tube on hoop strain. The fiber decreased the tube's hoop strain by 67% compared with that in non-strengthened tube. In the steel tube with 1-layer of GFRP, failure involved outward local buckling deformations near the ends and some inward buckling deformations developed in this specimen. In the control steel tube, the outward local buckling deformations was the only deformation developed in the specimen unlike the strengthened tube.

**Figure (6)** shows a comparison between the axial load-axial shortening curves obtained from both the experimental and numerical results. The figure shows good agreement between results of experimental tests and those obtained by the proposed ANSYS model. From the curve, it is obvious that FRP confinement of steel tubes leads to increase in ductility but limited improvement in the ultimate load. In ANSYS models, Shell 93 and Shell 181 were used. In the experimental study [8], it was mentioned that the rupture of the fiber was at ultimate strain equal 0.0228. **Figure (6)** showed that the fiber rupture happened before the attainment of the peak load in experimental result similar to the result obtained from the Shell 181 ANSYS model. Therefore, the model that used Shell 181 was more accurate than the Shell 93 model unexpectedly (Shell 93 is 8-node structural shell and more accurate than Shell 181 which is 4-node shell element). It could be argued that Shell 181 element is more consistent (than Shell 93) for the utilized values of imperfection parameters.

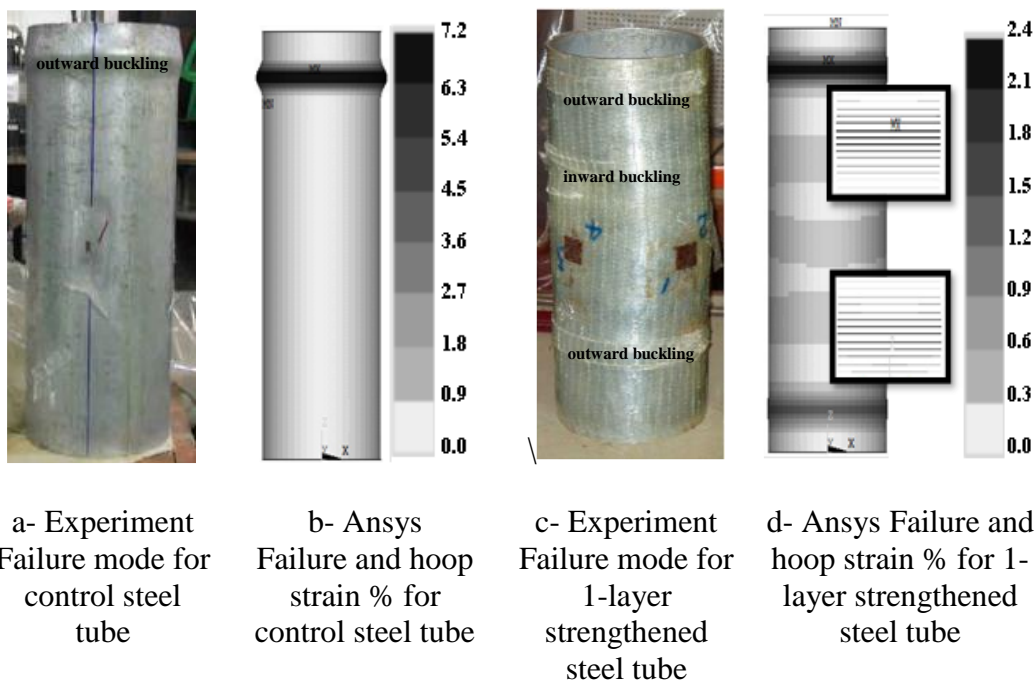


Fig. 5: Deformation of steel tube

**Figure (7)** shows the difference between the lateral displacement and axial displacement in control steel tube model and strengthened one, respectively. These contours were computed from the substep at the maximum axial shortening. They show that the values of lateral displacement in strengthened steel tube are less than the values in the control steel tube. This is due to the confinement of the fiber. The axial displacement in the control steel tube had smaller value compared to the strengthened one. It means that the enhances the ductility of the steel tube.

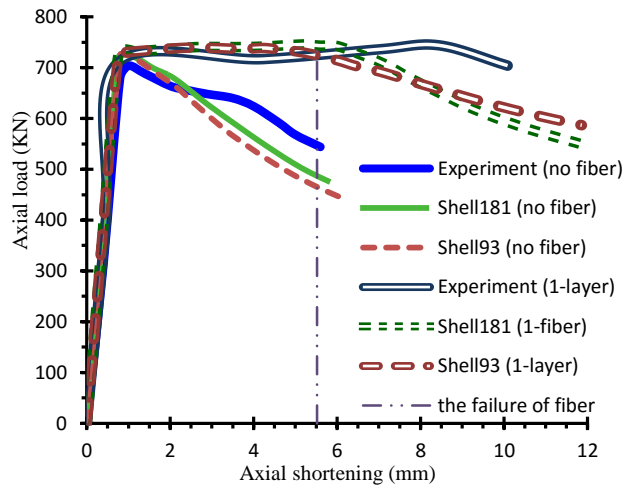


Fig. 6: Load vs. axial shortening for steel specimens

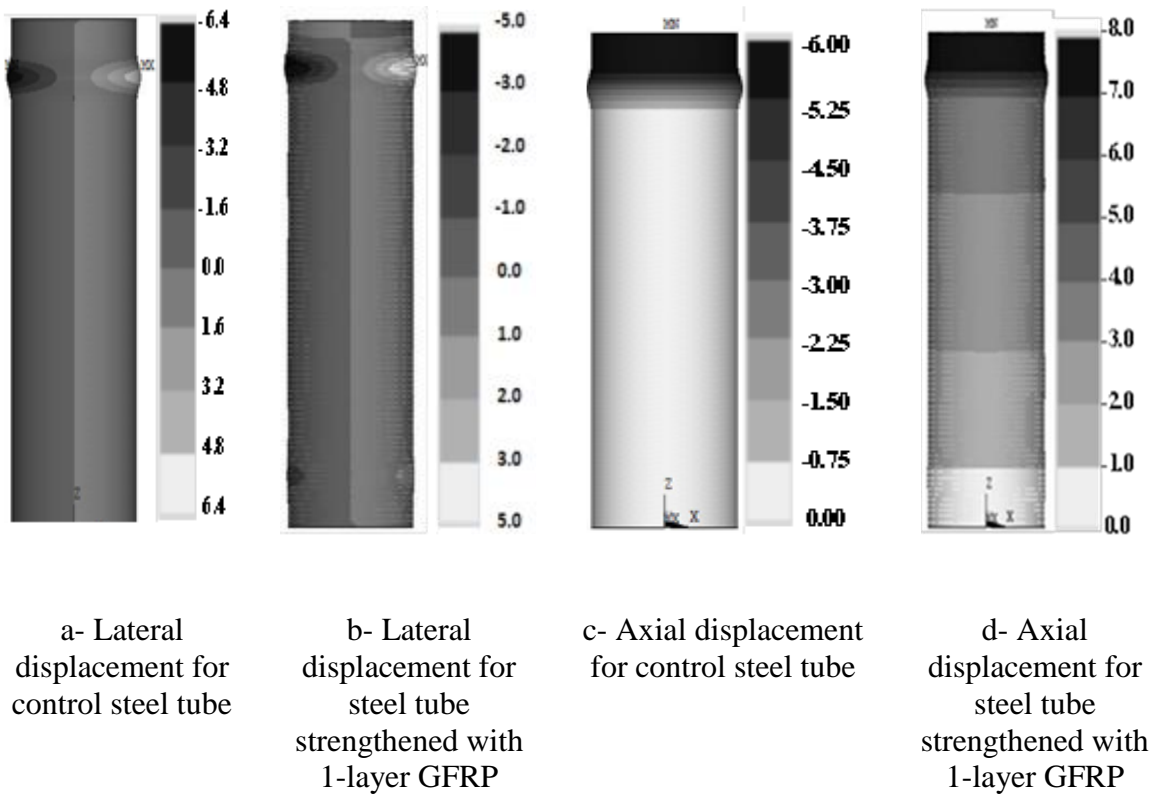


Fig. 7: Comparisons between the behavior of control steel tube and strengthened one

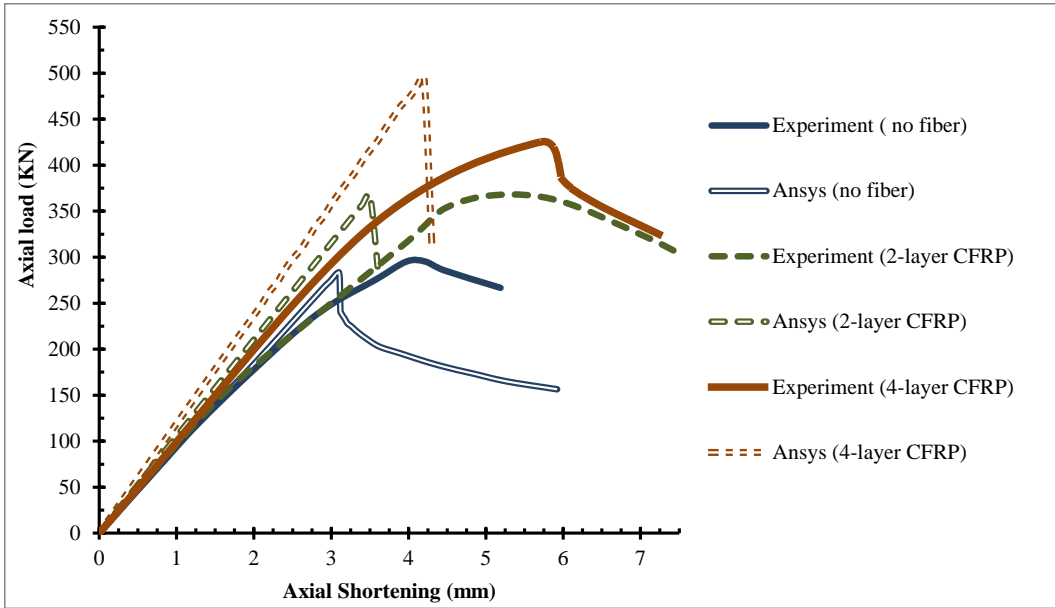
## 4.2 Overall buckling models

**Figure (8)** shows a comparison between the axial load-axial shortening curves and a comparison between the axial load-lateral displacement curves obtained from both the experimental and ANSYS model results, respectively. The figures show good agreement between results of experimental tests and those obtained by the proposed numerical model. The difference between the experimental and numerical curves came from the inconsistency of the imperfection values in experimental and numerical study. It is worth mentioning that the experimental imperfection values were not given in Ref. [10]. Therefore, a comparison was made between the results of a numerical analysis model mentioned in the source and the numerical results from ANSYS. The out-of-straightness imperfection values were mentioned as 2.4 mm. **Figure (9)** shows a comparison between the axial load-axial shortening curves and the axial load-lateral displacement curves obtained from the numerical results from the paper [10] and numerical results from ANSYS. From the curves, there was an increase in the axial load with almost same axial shortening and lateral displacement in the retrofitted specimens compared to control steel tube. It means that there was an increase in the strength of the tube. It can be noticed also that the initial slope of the curves of retrofitted steel tubes were higher than in the control steel tube. It was an indication that the CFRP layers have increased the axial stiffness and stability against lateral deflection.

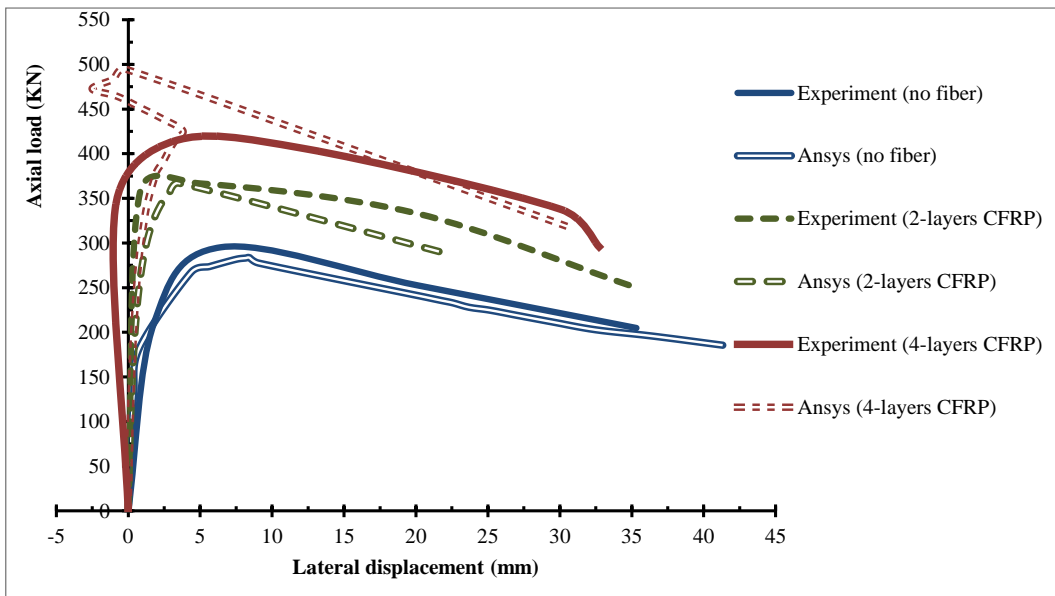
**Figure (10)** shows comparisons between the lateral displacement for the three models and the axial displacement for them respectively. It shows that the lateral displacement decreases in the retrofitted specimens by average 62% from its value at the control steel tube because of the CFRP confinement of the steel tube. They also show that the axial displacement decrease in the retrofitted specimens by about (45%) from its value at the control steel tube. These confirm that the usage of CFRP in strengthening of steel tube that exposure overall buckling enhances the strength of the steel and reduces the effect of the buckling.

## 5. Conclusions

This paper verified and evaluated the presented finite element models (made by ANSYS) by comparing their results to the experimental ones and to investigate the effect of strengthening on different modes of buckling. Two modes of buckling were studied; elephant's foot buckling mode and overall buckling mode. Through the results extracted from this study, the following conclusions are drawn:

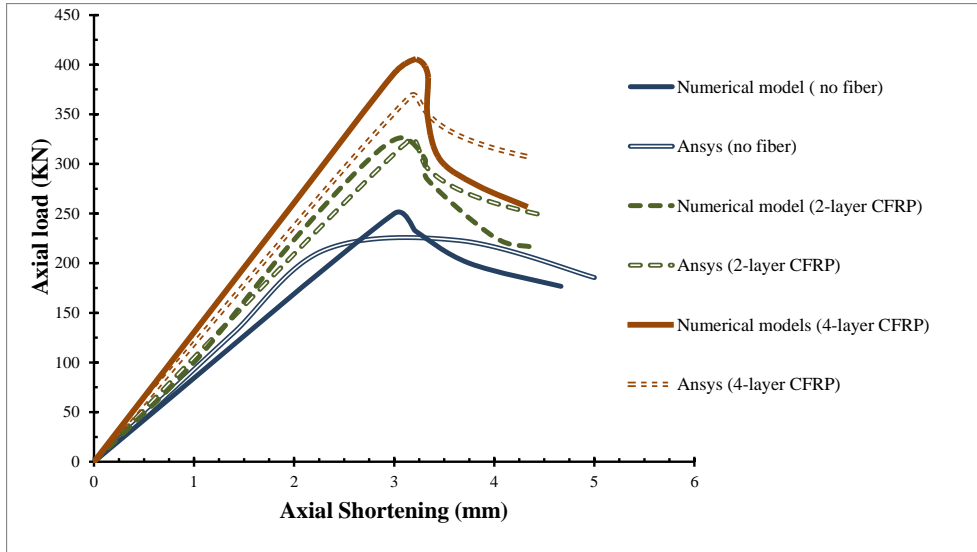


a- Load vs. axial shortening for steel specimens

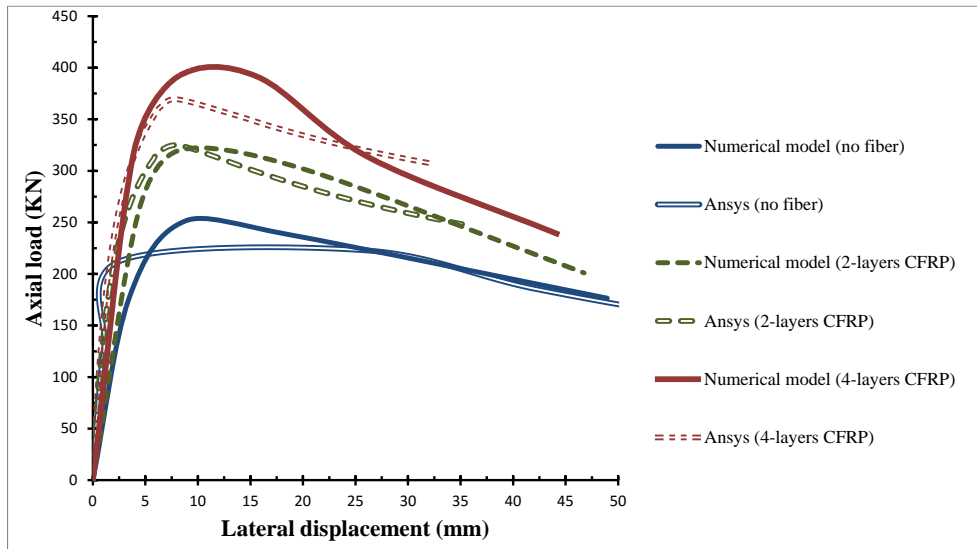


b- Load vs. lateral displacement for steel specimens

Fig. 8: Comparison between load vs. axial and lateral displacement in the experimental study (Gao et al., 2013) and in ANSYS models



a- Load vs. axial shortening for steel specimens



b- Load vs. lateral displacement for steel specimens

Fig. 9: Comparison between load vs. axial and lateral displacement in the numerical study (Gao et al., 2013) and in ANSYS models

- For the models studied elephant's foot buckling mode:
  1. The results of the developed finite element models show very good agreement with the experimental results available in the literature [11]. The behavior obtained from ANSYS model is very close to the experimental results.
  2. The GFRP strengthening enhances the ductility of the tubes with very little improvement in strength.

3. The strengthening with fiber decreases the lateral displacement of the tubes.
4. The employed shell finite element for modeling the steel tube is sensitive to the given imperfection values.

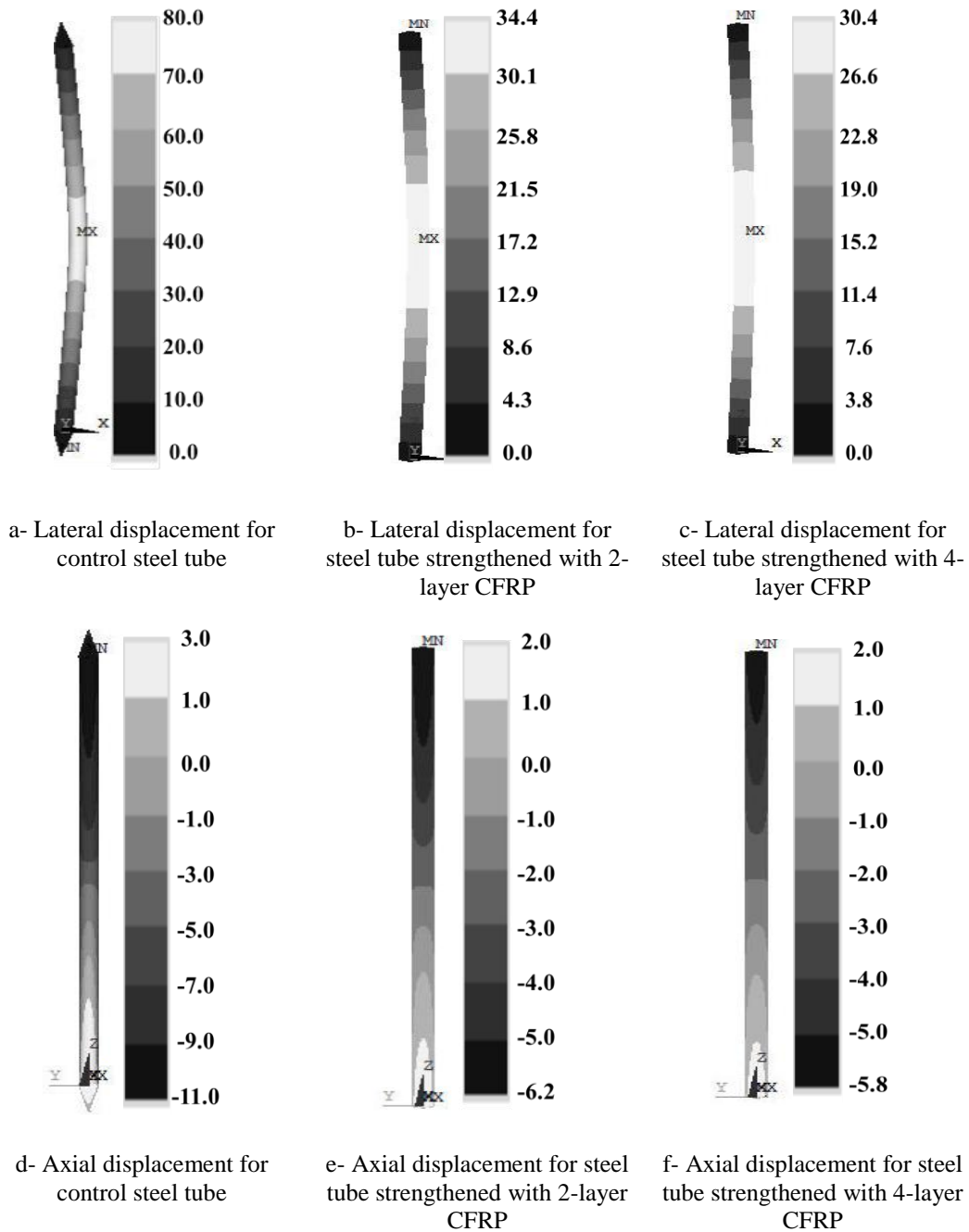


Fig. 10 Comparison between behavior of control and strengthened steel tube

The results of the developed finite element models show very good agreement with the experimental results available in the literature [11]. The behavior obtained from ANSYS model is very close to the experimental results.

- For the models studied overall buckling mode:
  1. The results of the developed finite element models show very good agreement with the experimental results available in the literature [10].
  2. Strengthening with CFRP causes great improvement on the strength and stiffness of the tube without any effect on the ductility.
  3. The strengthening with fiber decreases the lateral displacement of the tubes.

## REFERENCES

- 1- Agarwal D. S., Chhatwani A. C., "The Economic and Structural Analysis of Hollow Structural Sections", *International Journal on Recent and Innovation Trends in Computing and Communication*, V.3, P. 57-62, 2015.
- 2- Haedir J., Zhao X. L., "Design of Short CFRP-Reinforced Steel Tubular Columns", *Journal of Constructional Steel Research*, V. 67, P. 497-509, 2011.
- 3- Teng J. G., Yu T., Fernando D., "Strengthening of Steel Structures with Fiber-Reinforced Polymer Composites", *Journal of Constructional Steel Research*, V. 78, P. 131–143, 2012.
- 4- Alwash N. A., AL-Salih H. I., " Experimental Investigation on Behavior of SCC Filled Steel Tubular Stub Columns Strengthened with CFRP" , *Construction Engineering* , V. 1, P. 37-51, 2013.
- 5- Wang J., Afshan S., Schillo N., Theofanous M., Feldmann M., Gardner L., " Material Properties and Compressive Local Buckling Response of High Strength Steel Square and Rectangular Hollow Sections", *Engineering Structure*, V. 130, P. 297-315, 2017.
- 6- Šmak M., Straka B., "Geometrical and Structural Imperfections of Steel Member Systems", *Procedia Engineering*, V. 40, P. 434- 439, 2012.
- 7- Duggan M. F., "A Study of the Effects of Geometric Imperfection Upon the Stability Behavior of Cylindrical Shells under Axial Compression.", PhD diss., Georgia Institute of Technology, 1971.
- 8- El-Kholy, A. M., Morsy, U. A., Mourad, S. A., "Imperfection Modeling Using Finite Element Approach with Particular Discretization", *Journal of Structural Engineering*, V. 140(7), P. 04014034, 2014.
- 9- Shaat A., Fam A., "Axial Loading Tests on Short and Long Hollow Structural Steel Columns Retrofitted Using Carbon Fibre Reinforced Polymers", *Canadian Journal of Civil Engineering*, V. 33, P. 458-470, 2006.
- 10- Gao X.Y., Balendra T., Koh C.G., " Buckling Strength of Slender Circular Tubular Steel Braces Strengthened by CFRP", *Engineering Structures*, V. 46, P. 547–556, 2013.
- 11- Teng J. G., Hu Y. M., "Behaviour of FRP-Jacketed Circular Steel Tubes and Cylindrical Shells under Axial Compression", *Construction and Building Materials*, V. 21, P. 827–838, 2007.
- 12- GangaRao H. V. S., Vijay P. V., "Feasibility Review of FRP Materials for Structural Applications", Report, West Virginia University, USA, 2010.
- 13- Susana C.F., "Fiber Reinforced Polymer Composite Materials Used in Civil Engineering", Technical report, Structural and Repair Materials, Smart & Green, Portugal, 2008.

- 14- Batikha, M., Chen, J. F., Rotter, J. M., Teng, J. G., "Strengthening Metallic Cylindrical Shells Against Elephant's Foot Buckling with FRP", *Thin-Walled Structures*, V. 47, P. 1078-1091, 2009.
- 15- Haedir J., Zhao X. L., "Design of Short CFRP-Reinforced Steel Tubular Columns", *Journal of Constructional Steel Research*, V. 67, P. 497-509, 2011.
- 16- Nishino T., Furukawa T., "Strength and Deformation Capacities of Circular Hollow Section Steel Member Reinforced with Carbon Fiber", In *Proceedings of 7th Pacific Structural Steel Conference*, American Institute of Steel Construction, 2004.
- 17- ANSYS, "ANSYS Finite Elements Analysis Manual", SAS IP, Inc., PA, USA, 2009.
- 18- Mohammed, Y. A., "Strengthening of Tubular Steel Compression Members with Fiber- Reinforced Polymers (FRP)", M.Sc. Thesis, Fayoum University, 2018 (under preparation).